Journal of Materials Chemistry A

COMMUNICATION

View Article Online
View Journal | View Issue

Hierarchical structure $LiFePO_4$@C synthesized by oleylamine-mediated method for low temperature applications†

Cite this: *J. Mater. Chem. A*, 2014, **2**, 4870

Received 16th December 2013
Accepted 14th January 2014

DOI: 10.1039/c3ta15210c

www.rsc.org/MaterialsA

Jingmin Fan, Jiajia Chen, Yongxiang Chen, Haihong Huang, Zhikai Wei, Ming-sen Zheng* and Quanfeng Dong*

In this paper, a hierarchical nanostructure $LiFePO_4$@C composite was firstly fabricated by an oleylamine mediated method. The oleylamine played a multifunctional role in restricting the particle size and forming the porous nano-structure of $LiFePO_4$@C composite. Benefiting from its hierarchical structure, $LiFePO_4$@C exhibited superior electrochemical performance, especially at low temperature. It can deliver a capacity of 117 mA h g^{-1} at a current density of up to 700 mA g^{-1} (about 5 C) at −20 °C.

Since Padhi's work in 1997,[1] olivine-type lithium transition-metal phosphates have attracted considerable attention as one of the most promising lithium ion battery cathode materials for electric vehicles (EVs), plug-in hybrid electric vehicles (HEVs) and green grid, owing to their high theoretical capacity (~170 mA h g^{-1}), durability, thermal safety and low cost.[2–5] However, comparing to the high electrical conductivity of $LiCoO_2$ (10^{-3} S cm^{-1}) and $LiMn_2O_4$ (10^{-5} S cm^{-1}),[6] $LiFePO_4$ has a low electrical conductivity (10^{-9} S cm^{-1})[7] and sluggish lithium ion diffusion kinetics (at least three orders of magnitude lower than $LiCoO_2$). Numerous efforts have been paid to overcome these deficiencies, such as conductive materials coating (such as: carbon,[8] polymer,[9–11] poorly crystallized pyrophosphate[12]), doping[6,13–15] and minimizing the particle size.[16,17] According to these strategies, various methods (such as solid state reaction,[12] polyol and solvothermal,[18,19] hydrothermal,[20] ionothermal,[21] supercritical,[22] microwave-assisted,[23] electrospinning,[24] biological,[25] and spray pyrolysis[26]) have been developed to synthesize $LiFePO_4$ with different nanostructures. Nanosized particles can provide both a shorter diffusion pathway and a larger surface area for charge transfer. The nanoporous electrode can benefit the immersion of electrolyte, and these efforts lead to successful commercialization of $LiFePO_4$ with viable electrochemical performance. There have been several reports on $LiFePO_4$ with ultrahigh rate performance (up to 100 C) at room temperature.[12,27] However, it is still a challenge for $LiFePO_4$ to achieve a considerable electrochemical performance at low temperature, which impedes the practical application of electric vehicles in the winter or in cold areas. To date, $LiFePO_4$ are still difficult to operate at rate >1 C, when the temperature falls below −20 °C.

Herein, a $LiFePO_4$@C hierarchical structure with a superior low temperature electrochemistry performance is firstly synthesized by an oleylamine-mediated strategy. The hierarchical $LiFePO_4$@C cathode exhibited a superior electrochemical performance. It can deliver a specific capacity of 149, 140, 124 and 107 mA h g^{-1} at 5, 10, 50 and 100 C at room temperature, respectively. Moreover, the as-prepared $LiFePO_4$@C cathode can deliver a capacity of 117 mA h g^{-1} at a current density of 700 mA g^{-1}(about 5 C) when the temperature drops to −20 °C. As shown in Scheme 1, the nano-size pristine $LiFePO_4$ particles with a uniformly oleylamine coating shell were produced in the first solvothermal procedure. Then, the oleylamine converts to a uniformly carbon shell during the subsequent sintering step, forming an $LiFePO_4$@C composite. The carbon shell improves conductivity of the electrode and prevents agglomeration of

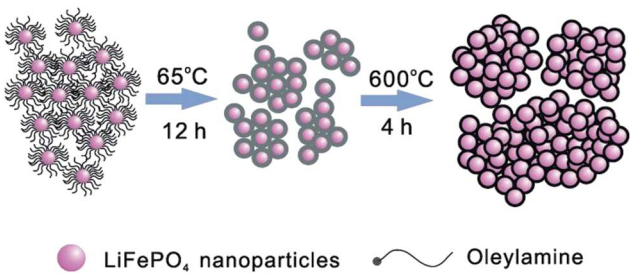

Scheme 1 Preparation process of the nano-$LiFePO_4$@C composite.

Department of Chemistry, College of Chemistry and Chemical Engineering, Xiamen University, State Key Laboratory of Physical Chemistry of Solid Surfaces, Xiamen, Fujian, 361005, P.R. China. E-mail: qfdong@xmu.edu.cn; mszheng@xmu.edu.cn; Fax: +86 0592-2183905; Tel: +86 0592-2185905

† Electronic supplementary information (ESI) available: Experimental details, material characterization, electrochemical measurements, Raman spectrum, additional electrochemical data and charge/discharge curve. See DOI: 10.1039/c3ta15210c

nano $LiFePO_4$. Finally, a hierarchical $LiFePO_4$@C composite was achieved from the self-assembly of $LiFePO_4$@C nanoparticles on the micrometer scale with a porous structure.

The size, morphology and crystal structure of the products were investigated by high resolution transmission electron microscopy (HRTEM), scanning electron microscopy (SEM) and X-ray diffraction (XRD). As shown in Fig. 1a and b, $LiFePO_4$@C composite after sintering consisted of mono-dispersed primary nanoparticles up to 30 nm, assembling into micrometer-scale particles. A thin carbon shell within 2 nm coating uniformly on the $LiFePO_4$ particles can be observed in the TEM image (Fig. 1c). D and G bands of carbon occurring at 1345 and 1594 cm^{-1} confirm that oleylamine can be carbonized during the sintering process and the average carbon content is determined to be 6.7 wt% using CHN element analysis (Fig. S1†). The porous structure and the Brunauer–Emmett–Teller (BET) surface area of $LiFePO_4$@C were also investigated by N_2 adsorption–desorption experiments at 77 K (Fig. S2†). The BET surface area was measured as 81.5 $m^2\ g^{-1}$. The average pore diameter was as large as 6.2 nm, calculated from the desorption branch of the isotherm using the Barrett–Joyner–Halenda (BJH) method, which would favor electrolyte immersion. The high BET surface area and the narrow average pore would facilitate the diffusion of lithium ion within the hierarchical structure of $LiFePO_4$@C.[28] The XRD patterns of $LiFePO_4$@C (Fig. 1d) are broadened due to the nanoscale of particles and still match well the theoretical XRD patterns of $LiFePO_4$.

The electrochemical performance of $LiFePO_4$@C was examined by coin-type cells within 4.2–2.4 V and all capacities were calculated based on the mass of $LiFePO_4$. The $LiFePO_4$@C cathode exhibits a superior high-rate capability (Fig. 2a). It can deliver 72% capacity of its theoretical value when the rate is up to 100 C without severe polarization at room temperature (Fig. S3†). Even under an extremely high current density (200 C rate, corresponding to 34 000 mA g^{-1}), it was also able to deliver a substantial capacity of 80 mA h g^{-1}. This is among the highest values reported (Table S1†).[12,27] The as-prepared $LiFePO_4$@C cathode also exhibits excellent cycle stability. As shown in Fig. 2b, no obvious fading was observed over 300 cycles at 0.5 C (85 mA g^{-1}) and 10 C (1700 mA g^{-1}) rates. Furthermore, there was only 0.012% capacity fading per cycle when the current density was raised up to 20 C (3400 mA g^{-1}), and with almost 100% coulombic efficiency.

At present, it is believed that the battery performance of $LiFePO_4$ dropping drastically at low temperature should be due to the sluggish lithium ion diffusion kinetics, increasing internal resistance and electrolyte freezing.[29–31] As listed in Table S1,† the capacity of $LiFePO_4$ was no more than 100 mA h g^{-1} at −20 °C at only 1 C rate at presnet.[27,30–32] However, the as-prepared hierarchical nanostructure of $LiFePO_4$@C demonstrated an excellent electrochemical performance at low temperature. When tested under 0 °C and −20 °C, it can deliver capacities of 138 and 117 mA h g^{-1} at 5 C (current density of 700 mA g^{-1}), respectively. It should be noted that the charge current

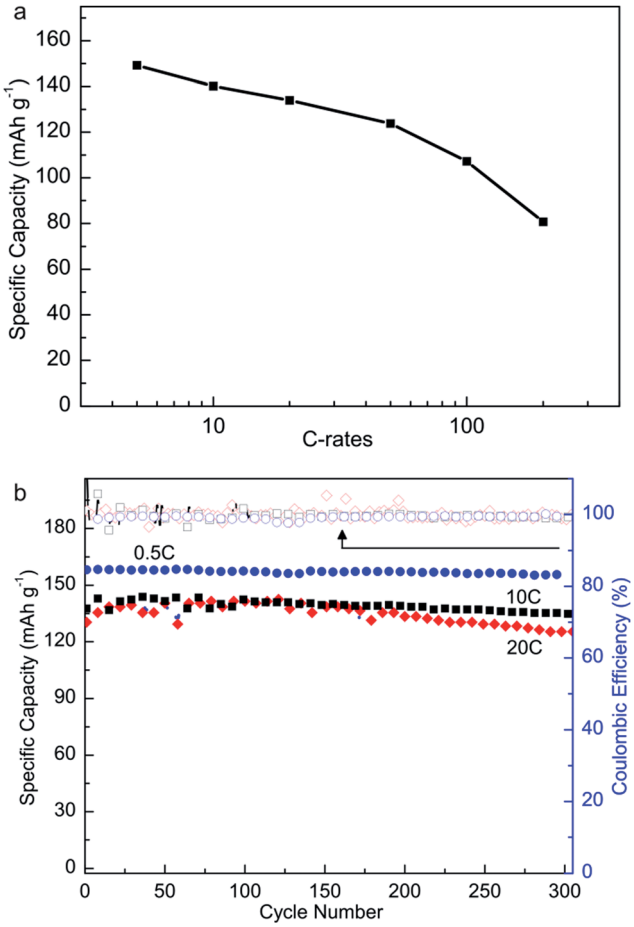

Fig. 2 (a) Rate performance of $LiFePO_4$@C at room temperature. (b) Cycling performance of $LiFePO_4$@C. 1 C = 170 mA g^{-1}.

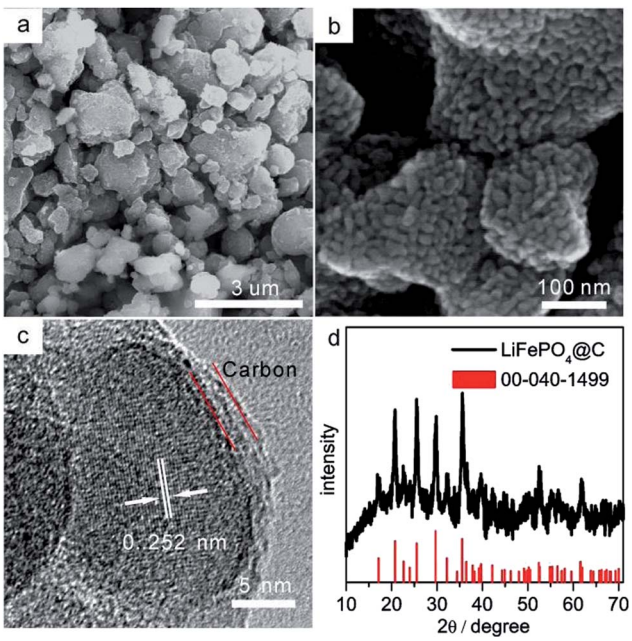

Fig. 1 Morphology characterization of $LiFePO_4$@C. (a and b) SEM images and (c) HRTEM image of $LiFePO_4$@C composite; (d) X-ray diffraction (XRD) patterns of $LiFePO_4$@C composite.

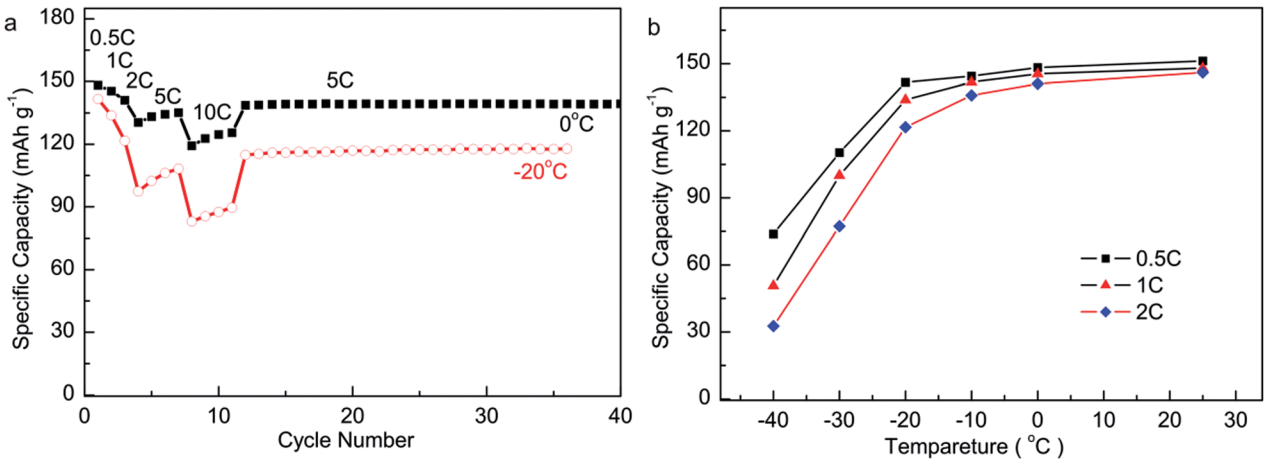

Fig. 3 (a) Discharge capacity *versus* cycle number plots of $LiFePO_4$@C from 0.5 C to 10 C and cycling at 5 C (700 mA g^{-1}) at 0 °C and −20 °C. (b) Discharge capacity at 0.5, 1 and 2 C at temperatures in the range of −40 ~ 25 °C.

density was the same as the discharge process, and both processes were performed at the same temperature. Furthermore, no capacity fading was found during the cycling at the 5 C rate, exhibiting an excellent stability at low temperature. To our best knowledge, this is the best result of a $LiFePO_4$ electrode at −20 °C.

To further understand the electrochemical kinetics of $LiFePO_4$@C composite, cyclic voltammetry (CV) and impedance measurements (EIS) were performed. ΔE_p between the anodic and cathodic peaks is only 0.13 V, which indicates a highly reversible redox reaction of $LiFePO_4$@C during the intercalation and deintercalation process at room temperature (Fig. S7†). Electrochemical impedance measurements of the $LiFePO_4$@C electrode at different temperatures were performed and fitted by using an equivalent circuit model (Fig. S8†). The semicircle in the middle frequency range corresponds to the charge transfer resistance (R_{ct}) while the sloping line in the lower frequency represents Li ion Warburg diffusion.[33] The impedance parameters derived using an equivalent circuit model and diffusion coefficient are listed in Table S2.†

R_{ct} increased from 11.73 Ω at 25 °C to 9258 Ω at −40 °C, abiding the Arrhenius equation. The Arrhenius activation energy is calculated to be 59.35 kJ mol^{-1} (Fig. S9†). High activation energy means that the charge transfer process is influenced greatly by temperature. The linear relationship between $1000/T$ and $\ln(1/R_{ct})$ indicates that the electrode/electrolyte interface can be well retained even at −40 °C. The diffusion coefficients at various temperatures according to the Warburg diffusion area of EIS results, are estimated as 3.93×10^{-12} cm^2 s^{-1} at 25 °C and 9.23×10^{-15} cm^2 s^{-1} at −20 °C, respectively. And the diffusion time for Li^+ diffuse over 30 nm (the particle size of as-prepared $LiFePO_4$) can be estimated as ~10 s and ~1000 s at 25 °C and −20 °C respectively, according to equation $t = L^2/D_{Li+}$ (L is the particle size). These were consistent with the electrochemical results (200 C at 25 °C, around 9 s and 2 C at −20 °C, around 1300 s). The diffusion coefficients demonstrate that the limiting step of as-prepared $LiFePO_4$@C at a high rate is the Li^+ diffusion kinetics in the bulk phase rather than the interface. When the temperature is higher than −20 °C, $LiFePO_4$@C still has the ability to retain a considerable battery performance (Fig. 3a and b). As the temperature drops below −20 °C, the capacities of the as-prepared $LiFePO_4$@C electrode steeply decreased from 121 mA h g^{-1} at −20 °C to 32 mA h g^{-1} at −40 °C at a current density of 2 C. The D_{Li+} no longer meets the Arrhenius equation when the temperature drops below −20 °C (Fig. S11†), suggesting a more restricted electrochemical kinetics occurred. This might result from the low lithium ion diffusion coefficient in the electrolyte.[34]

In summary, the superior kinetic character of the as-prepared $LiFePO_4$@C electrode is benefiting from its special structure: (1) hierarchical nanostructure constituted by particles and pores in different nano-scale; (2) every particle in the hierarchical structure is in the nano-scale within 30 nm; (3) every particle in the hierarchical structure is uniformly coated with a 2 nm carbon shell. Due to its porous structure, uniform carbon coating and nanosized particle, the as-prepared $LiFePO_4$@C electrode shows a superior electrochemical performance, especially at low temperature, which is an important factor for the practical applications of EVs/HEVs in winter. Moreover, this method can be easily extended to synthesize other energy storage materials such as $LiMnPO_4$.

Acknowledgements

The authors gratefully acknowledge financial support from the Key Project of NSFC (U1305246, 21321062), and the Major Project funded by Xiamen city (3502Z20121002).

Notes and references

1 A. K. Padhi, K. S. Nanjundaswamy and J. B. Goodenough, *J. Electrochem. Soc.*, 1997, **144**, 1188–1194.
2 M. Armand and J. M. Tarascon, *Nature*, 2008, **451**, 652–657.
3 B. Dunn, H. Kamath and J. M. Tarascon, *Science*, 2011, **334**, 928–935.

4 Z. Yang, J. Zhang, M. C. W. Kintner-Meyer, X. Lu, D. Choi, J. P. Lemmon and J. Liu, *Chem. Rev.*, 2011, **111**, 3577–3613.
5 L.-X. Yuan, Z.-H. Wang, W.-X. Zhang, X.-L. Hu, J.-T. Chen, Y.-H. Huang and J. B. Goodenough, *Energy Environ. Sci.*, 2011, **4**, 269–284.
6 S.-Y. Chung, J. T. Bloking and Y.-M. Chiang, *Nat. Mater.*, 2002, **1**, 123–128.
7 D. W. Choi, D. H. Wang, I. T. Bae, J. Xiao, Z. M. Nie, W. Wang, V. V. Viswanathan, Y. J. Lee, J. G. Zhang, G. L. Graff, Z. G. Yang and J. Liu, *Nano Lett.*, 2010, **10**, 2799–2805.
8 J. Wang and X. Sun, *Energy Environ. Sci.*, 2012, **5**, 5163–5185.
9 K. S. Park, S. B. Schougaard and J. B. Goodenough, *Adv. Mater.*, 2007, **19**, 848–851.
10 Y. H. Huang and J. B. Goodenough, *Chem. Mater.*, 2008, **20**, 7237–7241.
11 D. Lepage, C. Michot, G. X. Liang, M. Gauthier and S. B. Schougaard, *Angew. Chem., Int. Ed.*, 2011, **50**, 6884–6887.
12 B. Kang and G. Ceder, *Nature*, 2009, **458**, 190–193.
13 N. Meethong, Y.-H. Kao, S. A. Speakman and Y.-M. Chiang, *Adv. Funct. Mater.*, 2009, **19**, 1060–1070.
14 C. A. J. Fisher, V. M. H. Prieto and M. S. Islam, *Chem. Mater.*, 2008, **20**, 5907–5915.
15 F. Omenya, N. A. Chernova, S. Upreti, P. Y. Zavalij, K.-W. Nam, X.-Q. Yang and M. S. Whittingham, *Chem. Mater.*, 2011, **23**, 4733–4740.
16 C. Delacourt, P. Poizot, S. Levasseur and C. Masquelier, *Electrochem. Solid-State Lett.*, 2006, **9**, A352–A355.
17 R. Malik, D. Burch, M. Bazant and G. Ceder, *Nano Lett.*, 2010, **10**, 4123–4127.
18 T. Azib, S. Ammar, S. Nowak, S. Lau-Truing, H. Groult, K. Zaghib, A. Mauger and C. M. Julien, *J. Power Sources*, 2012, **217**, 220–228.
19 D. Rangappa, K. Sone, T. Kudo and I. Honma, *J. Power Sources*, 2010, **195**, 6167–6171.
20 B. Ellis, W. H. Kan, W. R. M. Makahnouk and L. F. Nazar, *J. Mater. Chem.*, 2007, **17**, 3248–3254.
21 N. Recham, L. Dupont, M. Courty, K. Djellab, D. Larcher, M. Armand and J. M. Tarascon, *Chem. Mater.*, 2009, **21**, 1096–1107.
22 D. Rangappa, K. Sone, M. Ichihara, T. Kudo and I. Honma, *Chem. Commun.*, 2010, **46**, 7548–7550.
23 I. Bilecka, A. Hintennach, I. Djerdj, P. Novak and M. Niederberger, *J. Mater. Chem.*, 2009, **19**, 5125–5128.
24 C. B. Zhu, Y. Yu, L. Gu, K. Weichert and J. Maier, *Angew. Chem., Int. Ed.*, 2011, **50**, 6278–6282.
25 Y. J. Lee, H. Yi, W. J. Kim, K. Kang, D. S. Yun, M. S. Strano, G. Ceder and A. M. Belcher, *Science*, 2009, **324**, 1051–1055.
26 J. Liu, T. E. Conry, X. Song, M. M. Doeff and T. J. Richardson, *Energy Environ. Sci.*, 2011, **4**, 885–888.
27 X.-L. Wu, Y.-G. Guo, J. Su, J.-W. Xiong, Y.-L. Zhang and L.-J. Wan, *Adv. Energy Mater.*, 2013, **3**, 1155–1160.
28 C. Kuss, D. Lepage, G. Liang and S. B. Schougaard, *Chem. Sci.*, 2013, **4**, 4223–4227.
29 X. H. Rui, Y. Jin, X. Y. Feng, L. C. Zhang and C. H. Chen, *J. Power Sources*, 2011, **196**, 2109–2114.
30 X.-Z. Liao, Z.-F. Ma, Q. Gong, Y.-S. He, L. Pei and L.-J. Zeng, *Electrochem. Commun.*, 2008, **10**, 691–694.
31 S. S. Zhang, K. Xu and T. R. Jow, *J. Power Sources*, 2006, **159**, 702–707.
32 S. W. Oh, S.-T. Myung, S.-M. Oh, K. H. Oh, K. Amine, B. Scrosati and Y.-K. Sun, *Adv. Mater.*, 2010, **22**, 4842–4845.
33 T. Muraliganth, A. V. Murugan and A. Manthiram, *J. Mater. Chem.*, 2008, **18**, 5661–5668.
34 E. J. Plichta and W. K. Behl, *J. Power Sources*, 2000, **88**, 192–196.